PEEC modeling of automotive electromagnetic problems

Giulio Antonini* G. Miscione* , J. Ekman+

* *UAq EMC Laboratory*

Dipartimento di Ingegneria Elettrica e dell'Informazione

Università degli Studi di L'Aquila

Monteluco di Roio, 67040 AQ, Italy

+ Department of Computer Science and Electrical Engineering,

Luleå University of Technology,

971 87 Luleå, Sweden

Abstract

This paper presents the combination of the nonorthogonal Partial Element Equivalent Circuit (PEEC) models and interconnect structures through a macromodel approach for the analysis of automotive electromagnetic problems. The applications are within automotive computational electromagnetics due to the typical combination of cable harnesses and chassis structures. It is shown that PEEC-based solvers are capable of handling electrically large problems with high geometrical complexity for detailed analysis in both the time- and frequency- domain with attached multi-conductor transmission lines.

Index Terms

Electromagnetic modeling, equivalent circuit, electromagnetic compatibility, macromodels

I. Introduction

The need for three-dimensional (3-D) electromagnetic (EM) modeling is increasing due to multi-gigahertz signal bandwidths at all levels of integration and packaging, mixed-signal functionality, and larger wiring densities in complex 3-D environments [1]. In the 2005 International Technology Roadmap for Semiconductors (ITRS) [2], the use of high frequency 3-D EM modeling is designated as an emerging area. Solving combined electromagnetic and circuit analysis problems is required for printed circuit board (PCB), subsystem-PCB modeling, and electrical interconnect and package (EIP) problems. Two-dimensional (2-D) multiconductor transmission line (MTL) analysis is used for problems which can be solved in this way. However, where 2-D modeling is inadequate, 3-D modeling techniques must be used. The partial element equivalent circuit (PEEC) method [3], [4], [5] is a 3-D full-wave

Corresponding Author: G. Antonini, *UAq EMC Laboratory*, Dipartimento di Ingegneria Elettrica, Università degli Studi di L'Aquila, Monteluco di Roio, 67040, L'Aquila, Italy. Tel.:+39-0862-434462, fax: +39-0862-434403, e-mail: antonini@ing.univaq.it

modeling method suitable for combined EM and circuit analysis. Unlike the method of moments (MoM), PEEC is a full spectrum method valid from dc to the maximum frequency determined by the meshing. In the PEEC method, the integral equation is interpreted as Kirchoff's voltage law applied to a basic PEEC cell, which results in a complete circuit solution for 3-D geometries. The equivalent circuit formulation allows for additional SPICE type circuit elements to be easily included. Further, the models and the analysis apply to both the time-and the frequency-domain. With a general purpose SPICE type solver, different analysis such as quasi-static, LR or RC, and multi-conductor transmission line model analysis can be performed.

The PEEC method has recently been extended to include nonorthogonal geometries [6]. This model extension, which is consistent with the classical orthogonal formulation, includes the Manhattan representation of the geometries in addition to the more general quadrilateral and hexahedral elements. This helps in keeping the number of unknowns at a minimum and thus reduces computational time for nonorthogonal geometries.

Electronic components and systems are widely used in modern vehicles for safety, control, and entertainment systems for example. While this revolution was going on, the electronics industry developed issues and concepts that were addressed to allow inter-operation of the systems in the presence of each other and with the external environment. For this reason electromagnetic compatibility (EMC) has gained an increasing importance as systems and components started to have influence on each other just due to their operation. The advent of electric and hybrid vehicles and the increasingly wide range of systems and frequencies which are used in vehicles, are expected to make automotive EMC an increasingly troublesome burden to vehicle manufacturers in the future. It is considered that the adoption of numerical modeling techniques will provide the most cost effective approach for future automotive EMC engineering. The PEEC method has shown to be particularly suitable for the solution of EMC and electrical interconnect and package (EIP) problems in combination with SPICE type circuit models since the entire problem is solved in the circuit domain. The advantage with the method is the systematic development of equivalent circuits which offers a good insight in the physics of the original problem and a deep understanding of the interaction mechanisms (conduction and radiation).

To efficiently handle the combination of complex PEEC models and interconnect structures (signal transmission in cable harnesses), the cables can not be meshed and treated as PEEC models. This would create an extremely large PEEC model which would result in excessive calculation times. Therefore, cable harnesses could be treated using multi-conductor transmission line (MTL) theory and integrated with the PEEC model. For example, work in this direction has been presented for transmission lines in [7]. In this work, the combination of PEEC models with MTL:s is conducted through a macromodel description. The MTL port voltages/current are related to PEEC model node potentials/currents and the two models are solved simultaneously. This gives a very efficient solution of the problem in both the time and frequency domain.

II. PEEC BASIC THEORY

The PEEC formulation uses an integral equation solution of Maxwell's equations based on the total electric field.

The starting point is the total electric field at or in the material which is:

$$\boldsymbol{E}^i(\boldsymbol{r},t) = \frac{\boldsymbol{J}(\boldsymbol{r},t)}{\sigma} + \frac{\partial \boldsymbol{A}(\boldsymbol{r},t)}{\partial t} + \nabla\phi(\boldsymbol{r},t) \tag{1}$$

where $\boldsymbol{E}^i$ is the incident electric field, $\boldsymbol{J}$ is the current density in a conductor and $\boldsymbol{A}$ and ϕ are vector and scalar potentials respectively. The vector potential $\boldsymbol{A}$ is for a single conductor at the field point $\boldsymbol{r}$ given by:

$$\boldsymbol{A}(\boldsymbol{r},t) = \mu \int_{v'} G(\boldsymbol{r},\boldsymbol{r}')\boldsymbol{J}(\boldsymbol{r}',t_d)dv' \tag{2}$$

The scalar potential is similarly

$$\phi(\boldsymbol{r},t) = \frac{1}{\epsilon_0} \int_{v'} G(\boldsymbol{r},\boldsymbol{r}')\varrho(\boldsymbol{r}',\tau)dv' \tag{3}$$

where the free space Green's function is

$$G(\boldsymbol{r},\boldsymbol{r}') = \frac{1}{4\pi} \frac{1}{\mid \boldsymbol{r}-\boldsymbol{r}' \mid} \tag{4}$$

and the retardation time is given by $\tau = t - \frac{|\boldsymbol{r}-\boldsymbol{r}'|}{c}$ which simply is the free space travel time between the points $\boldsymbol{r}$ and $\boldsymbol{r}'$. The conservation of charge is enforced by the continuity equation:

$$\nabla \cdot \boldsymbol{J}\left(\boldsymbol{r},t\right) = -\frac{\partial \varrho\left(\boldsymbol{r},t\right)}{\partial t} \tag{5}$$

The most popular method for the discretization of integral equations was called by Harrington the *method of moments* (MoM) [8] with different implementation [9]-[12]. In PEEC, in the first step the unknown quantities $\boldsymbol{J}\left(\boldsymbol{r},t\right)$ and $\varrho\left(\boldsymbol{r},t\right)$ are expanded as a weighted sum of finite set of basis functions. Next, the so-called Galerkin's testing or weighting process ([13]) is used to generate a system of equations for the unknowns weights by enforcing the residuals of equations (1)-(5) to be orthogonal to a set of weighting functions which are chosen to be coincident with the basis functions. It is evident that this procedure transforms equations (1)-(5) into the Kirchoff Voltage and Current Laws (KVL and KCL) respectively.

A. Improved PEEC models for accuracy and stability

In the PEEC framework, the magnetic field coupling between two elementary volumes α and β is described by partial inductances defined, in the Laplace domain, as:

$$L_{p,\alpha\beta}(s) = \frac{\mu_0}{4\pi a_\alpha a_\beta} \int_{v_\alpha}\int_{v_\beta} \frac{e^{-s\tau}}{|\boldsymbol{r}_\alpha - \boldsymbol{r}_\beta|} \boldsymbol{u}_\alpha \cdot \boldsymbol{u}_\beta \; dv_\alpha dv_\beta \tag{6}$$

where $\tau = |\boldsymbol{r}_\alpha - \boldsymbol{r}_\beta|/c_0$ and c_0 is the speed of light in vacuum. In the past such coefficient was approximated taking the exponential term out of the integral. More recently [14] it has been pointed out that such choice may prevent the model to capture the damping which occurs at high frequency, causing inaccuracies and late-time instability. For this reason a macromodel for the partial element has been evaluated, providing accuracy and better stability properties at the same time [15]. These targets are achieved by means of different techniques based on: (1) subdivision schemes [16], (2) *split-cap filter* [15], (3) *R-ind filter* [15], and (4) macromodels generated by orthogonal vector fitting techniques [17] which will be described in detail in the references.

B. Non-orthogonal formulation

Three dimensional electromagnetic modeling of car chassis requires handling non-orthogonal geometries. The PEEC formulation for non-orthogonal geometry utilizes a *global* as well as a *local* coordinate system. The key *global* coordinate system uses conventional orthogonal coordinates x, y, z. Hence, a global vector $\boldsymbol{F}$ is of the form $\boldsymbol{F} = F_x\hat{\boldsymbol{x}} + F_y\hat{\boldsymbol{y}} + F_z\hat{\boldsymbol{z}}$. Therefore, the global unit vectors $\hat{\boldsymbol{x}}$, $\hat{\boldsymbol{y}}$ and $\hat{\boldsymbol{z}}$ are position independent. A vector in the global coordinates is denoted as $\boldsymbol{r}$. All local coordinates have to relate back to the global x, y, z coordinates. Therefore, a unique representation is needed for the mapping from a local point a, b, c on an object to the global point $\boldsymbol{r_g}$. Mapping a point in the above hexahedron from a local coordinate point a, b, c into a global coordinate point x, y, z is described by $x = \sum_{k=0}^{7} N_k(a, b, c)x_k$, which is applied for $x = x, y, z$ with coefficients given by

$$
\begin{aligned}
N_0 &= 1/8(1-a)(1-b)(1-c) \qquad & N_1 &= 1/8(1-a)(1-b)(1+c) \\
N_2 &= 1/8(1-a)(1+b)(1-c) \qquad & N_3 &= 1/8(1-a)(1+b)(1+c) \\
N_4 &= 1/8(1+a)(1-b)(1-c) \qquad & N_5 &= 1/8(1+a)(1-b)(1+c) \\
N_6 &= 1/8(1+a)(1+b)(1-c) \qquad & N_7 &= 1/8(1+a)(1+b)(1+c)
\end{aligned}
\tag{7}
$$

where $a \in [-1, +1]$ and again $a = a, b, c$.

Fig. 1 (a) details the (Lp,P,τ)PEEC model for the nonorthogonal metal patch in Fig. 1 (b) when discretized using four edge nodes (dark full circles). The model in Fig. 1 (a) consists of:

- partial inductances (Lp) which are calculated from the volume cell discretization using a double volume integral.
- coefficients of potentials which are calculated from the surface cell discretization using a double surface integral.
- retarded current controlled current sources, to account for the electric field couplings, given by $I_p^i = \frac{pij}{pii} I_C^j(t - t_{d_{ij}})$ where $t_{d_{ij}}$ is the free space travel time (delay time) between surface cells i and j,
- retarded current controlled voltage sources, to account for the magnetic field couplings, given by $V_L^n = Lp_{nm}\frac{\partial I_m(t-t_{d_{nm}})}{\partial t}$, where $t_{d_{nm}}$ is the free space travel time (delay time) between volume cells n and m.

III. PEEC-BASED ELECTROMAGNETIC SOLVER

A program for electromagnetic analysis, based on the theory and references outlined in the previous section, has been developed [18]. The solver can handle both the traditional orthogonal PEEC model and the newly introduced nonorthogonal formulation which is needed for the analysis of automotive problems. The solver creates an equivalent circuit containing resistances, inductances, capacitances, and coupled voltage and current sources (to account for electromagnetic couplings) for the given geometrical layout (CAD-data as specified in an input file). The user adds external electronic (sub-)systems and analysis mode as described by the SPICE syntax. For example, the solver performs transient analysis by the use of the `.tran`-command. The actual solution of the resulting circuit equations, in either the time- or frequency- domain, is performed in the solver and results are given as current- and voltage-distributions in the geometrical layout.

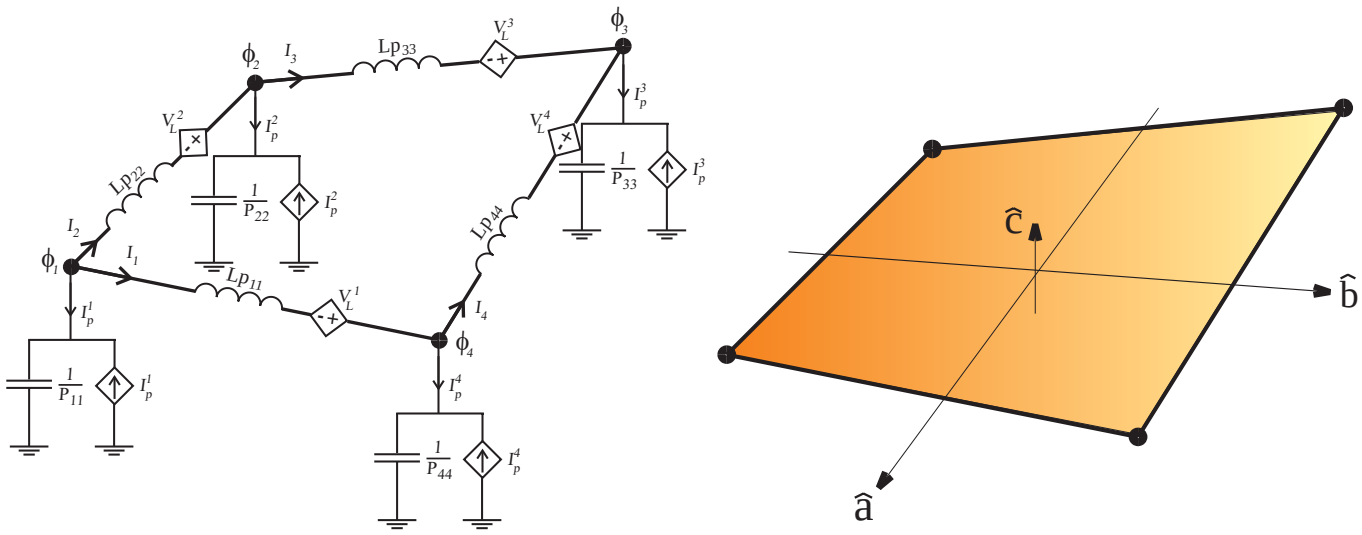

Fig. 1. Nonorthogonal metal patch (a) and PEEC model (b).

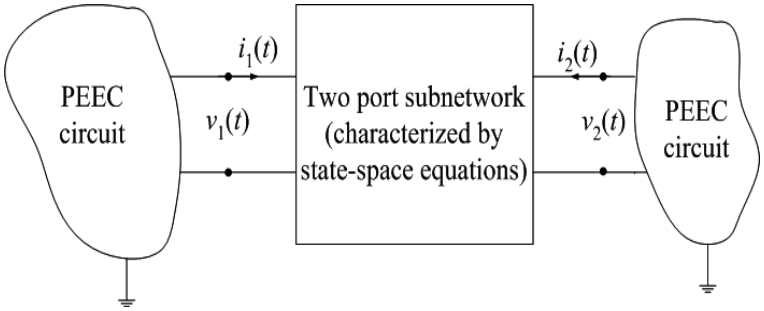

Fig. 2. PEEC model connected to a multiport system.

IV. Incorporation of Macromodels

Automotive computational electromagnetic problems can be extremely complex to be modeled entirely in the PEEC framework. Therefore, it can be useful to incorporate a macromodel describing an electromagnetic system into PEEC models. This can be accomplished by starting from a linear electromagnetic system described by a state-space model

$$\begin{cases} \dot{\boldsymbol{x}}(t) = \boldsymbol{A}\boldsymbol{x}(t) + \boldsymbol{B}\boldsymbol{v}(t) \\ \boldsymbol{i}(t) = \boldsymbol{C}\boldsymbol{x}(t) + \boldsymbol{D}\boldsymbol{v}(t) \end{cases} \tag{8}$$

where $\boldsymbol{A} \in \mathbf{R}^{p\times p}$, $\boldsymbol{B} \in \mathbf{R}^{p\times q}$, $\boldsymbol{C} \in \mathbf{R}^{q\times p}$, $\boldsymbol{D} \in \mathbf{R}^{q\times q}$, p is the number of states, q is the number of ports, $\boldsymbol{x}(t)$ is the state of the macromodel, and inputs and outputs are represented by the port voltages $\boldsymbol{v}(t)$ and the port currents $\boldsymbol{i}(t)$, respectively. Fig. 2 shows an example of the incorporation of a multiport system into the PEEC environment.

The discretization process of the EFIE (1) and the successive Galerkin's weighting leads to generate an equivalent circuit as seen in Fig. 1 (a). When Kirchhoff's voltage and current laws are enforced to the N_i independent loops

and N_ϕ independent nodes of the PEEC equivalent circuit we obtain:

$$-\boldsymbol{A}\boldsymbol{\Phi}\left(t\right)-\boldsymbol{R}\boldsymbol{i}_L\left(t\right)-\boldsymbol{L}_p\dot{\boldsymbol{i}}\left(t\right)=\boldsymbol{v}_s\left(t\right) \tag{9a}$$

$$\boldsymbol{P}^{-1}\dot{\boldsymbol{\Phi}}\left(t\right)+\boldsymbol{i}_{macro}-\boldsymbol{A}^t\boldsymbol{i}_L\left(t\right)=\boldsymbol{i}_s(t) \tag{9b}$$

where

- $\boldsymbol{\Phi}\left(t\right)\in\mathbf{R}^{N_\phi}$ is the vector of node potentials to infinity; $\mathbf{R}^{N_\phi}$ is the node space of the equivalent network;
- $\boldsymbol{i}_L\left(t\right)\in\mathbf{R}^{N_i}$ is the vector of currents including both conduction and displacement currents; $\mathbf{R}^{N_i}$ is the current space of the equivalent network;
- $\boldsymbol{i}_{macro}\left(t\right)\in\mathbf{R}^{N_\phi}$ is the vector of currents of macromodels;
- $\boldsymbol{L}_p$ is the matrix of partial inductances describing the magnetic field coupling;
- $\boldsymbol{P}$ is the matrix of coefficients of potential describing the electric field coupling;
- $\boldsymbol{R}$ is the matrix of resistances;
- $\boldsymbol{A}$ is the connectivity matrix;
- $\boldsymbol{v}_s(t)$ is the vector of distributed voltage sources due to external electromagnetic fields or lumped voltage sources;
- $\boldsymbol{i}_s(t)$ is the vector of lumped current sources.

The port voltages $\boldsymbol{v}(t)$ can be related to node potentials $\Phi(t)$ through the relation:

$$\boldsymbol{v}(t)=\boldsymbol{S}\Phi(t) \tag{10}$$

where $\boldsymbol{S}\in\mathbf{R}^{p\times N_\phi}$; it is easy to verify that, between macromodel currents $\boldsymbol{i}_{macro}\left(t\right)$ and port currents $\boldsymbol{i}\left(t\right)$ the following relation holds:

$$\boldsymbol{i}_{macro}\left(t\right)=\boldsymbol{S}^T\boldsymbol{i}\left(t\right) \tag{11}$$

that allows to map port currents into the N_ϕ PEEC nodes (dark circles in Fig. 1 (a) and (b)). Equations (9a)-(9b), (8), along with (10)-(11), represent a set of $N_i+N_\Phi+p+q$ equations to be solved for the same number of unknowns, namely $\boldsymbol{i}_L\left(t\right),\boldsymbol{\Phi}\left(t\right),\boldsymbol{x}\left(t\right),\boldsymbol{i}\left(t\right)$.

It is to be pointed out that the proposed approach allows to link multi-conductors transmission lines to PEEC models as well as any kind of macromodel of linear electromagnetic systems.

V. Numerical results for chassis structure

In the first test the developed PEEC solver has been used to analyze the voltage distribution on a car chassis in both the time- and frequency domain. The sequential PEEC-solver is written in C++, uses the GMM++ template library for matrix computation, and all the test are performed on a standard Linux server (Intel Xeon, duel core with 4 Gb RAM).

The discretization process, mesh seen in Fig. 4 (a), of the overall chassis structure into quadrilateral patches led to 3 816 inductive cells, 2 862 capacitive cells, and 1 355 nodes. This results in 14 558 040 mutual inductances,

8 188 182 mutual coefficients of potential (capacitances) which results in an $N \times N$ dense linear system $Ax = b$ with N = 5 171. This system is complex in the frequency domain due to the phase shift in the electromagnetic couplings while the time domain solver requires the use of history files for potentials and currents.

The majority of the computation time (4 hours), for both the tests, is the calculation of the nonorthogonal partial elements (inductances and coefficients of potential). The subsequent solution of the circuit equations is performed in 10 minutes in the time domain (1 500 time steps) and in 3 hours in the frequency domain (100 frequencies).

A. Time domain analysis

The first test is carried out in the time domain with the chassis excited by a fast current pulse. The current source is a pulse waveform of Gaussian-type, $I(t) = e^{-x \cdot x}$ where $x = \frac{t-(150e-9)}{(50e-9)}$, injected in the front bumper. The back bumper is terminated with a 50 Ω resistor to infinity in order to have a current path through the chassis. This results in the terminal voltages, at the front bumper (V_{FRONT}) and back bumper (V_{BACK}), as seen in Fig. 3 (a). The results, current and voltage distribution, can be visualized in the analyzed structure instead at single ports. This results in the potential distribution, in the chassis, as seen in Fig. 3 (b) for time $t = 180$ ns.

B. Frequency domain analysis

The only addition for the frequency domain test is a resistor (100 Ω) in parallel with the input current source (unitary for AC analysis). The result is given as the potential distribution in the chassis at 22 MHz in Fig. 4.

C. Chassis with and an interconnect structure

The second test adds a multi-conductor transmission line (MTL) to the chassis analysis in the previous section. The inclusion of the MTL is through the macromodel formulation detailed in Sec. IV. The interconnect structure consists of two signal lines with a common reference conductor, driving circuitry, and a PEEC model for two square loops as schematically shown in Fig. 5. The interconnect structure is positioned near the back window of the chassis, Fig. 6 (b).

For testing, one signal conductor is excited using a unitary Gaussian pulse function with a 5 ns rise time. The port voltages for the MTL is observed as well as the induced voltages and currents in the chassis.

The port voltages, near and far end, are shown in Fig. 6 (a). The induced voltages in the chassis, as seen in Fig. 6 (b), are close to 0.4 V near the small loop structures.

Since the proposed approach works well for frequency domain analysis, the last example shows a situation where a current- and voltage- distribution in the chassis impact on interconnect port voltages through the loop structures. The chassis is excited as described in Sec. 4.1.2 while observing the interconnect port voltages, seen in Fig. 7. Port voltages well over 1.5 V are observed around 85 MHz. Further, since the loop attached to signal conductor 2 is closer to the chassis, the induced voltages are slightly higher (Vin T2 and Vout T2 in Fig. 7) in that one than in signal conductor 1.

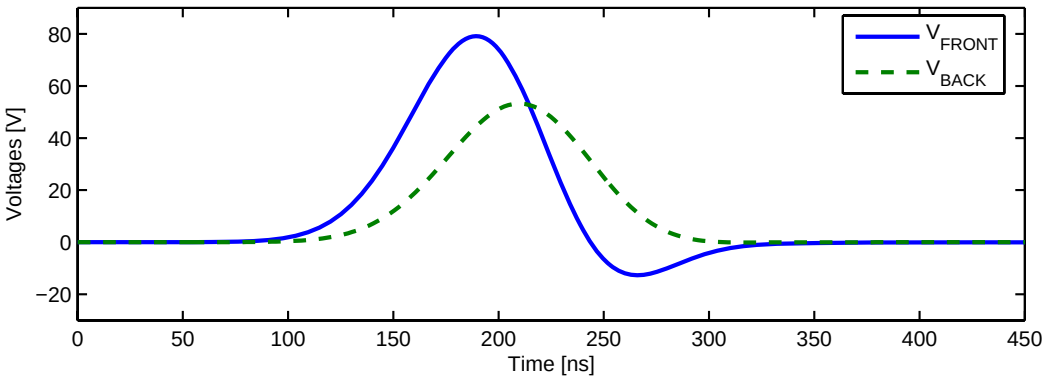

(a)

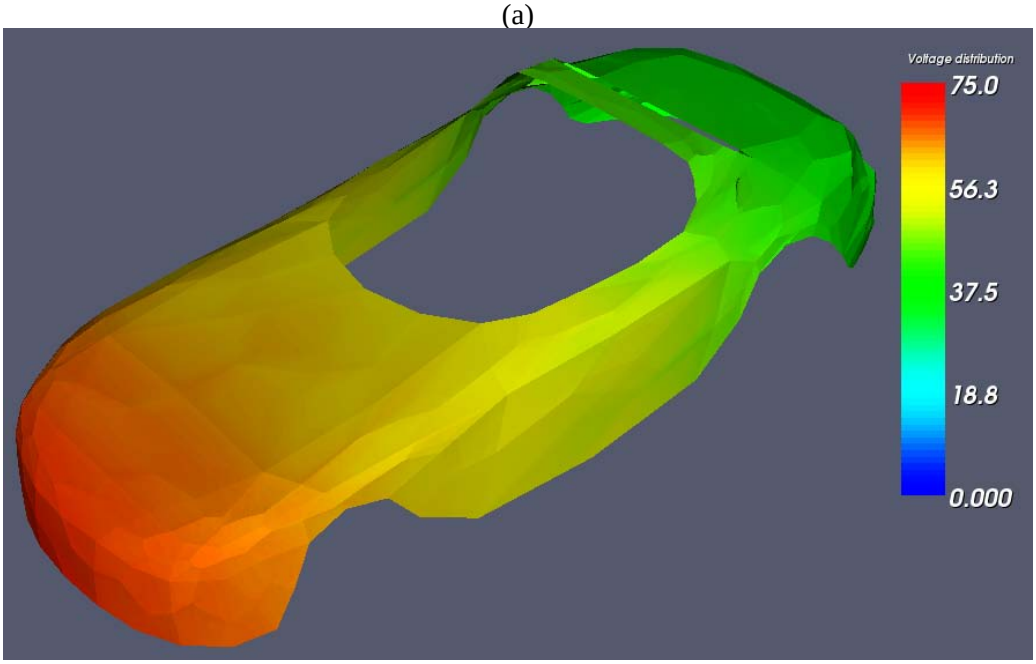

(b)

Fig. 3. Time domain voltages at front and back bumper of chassis for the current injection (a). Potential distribution in chassis at a specific time point (180 ns) after excitation with the Gaussian pulse.

The overall computation time, compared to single chassis analysis, is not impacted due to the addition of the macromodel and the loop circuits. This is due to the minimal inclusion of unknowns compared to the chassis structure. However, the creation of the macromodels require some effort in post-processing to create the $\boldsymbol{A}$, $\boldsymbol{B}$, $\boldsymbol{C}$, and $\boldsymbol{D}$ matrices in (8).

VI. Conclusions and Discussion

This paper shows the first application of nonorthogonal PEEC to an electrically large structure in both the time- and frequency domain. The developed solver is utilizing standard C++ libraries and requires only a Linux server to perform the analysis. Within the PEEC framework, additional active and passive circuit elements are easily included which enable the analysis if complete automotive systems with the effects of the chassis geometry in the same solver.

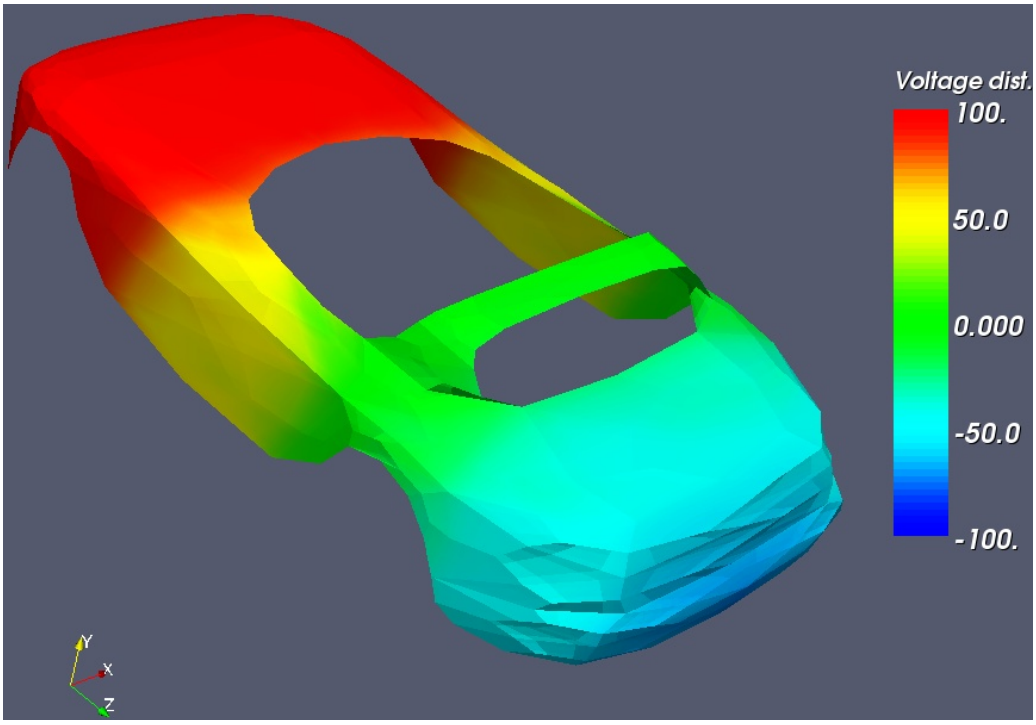

Fig. 4. Potential distribution in chassis analyzed with the PEEC solver at 22 MHz.

This paper also outlines the combination of PEEC models and interconnect structures through a macromodel approach. The applications are within automotive computational electromagnetics and involve nonorthogonal PEEC models for electrically large structures. With the electrically large structures, multi-conductor transmission lines are included through a macromodel approach resulting in an computationally efficient method.

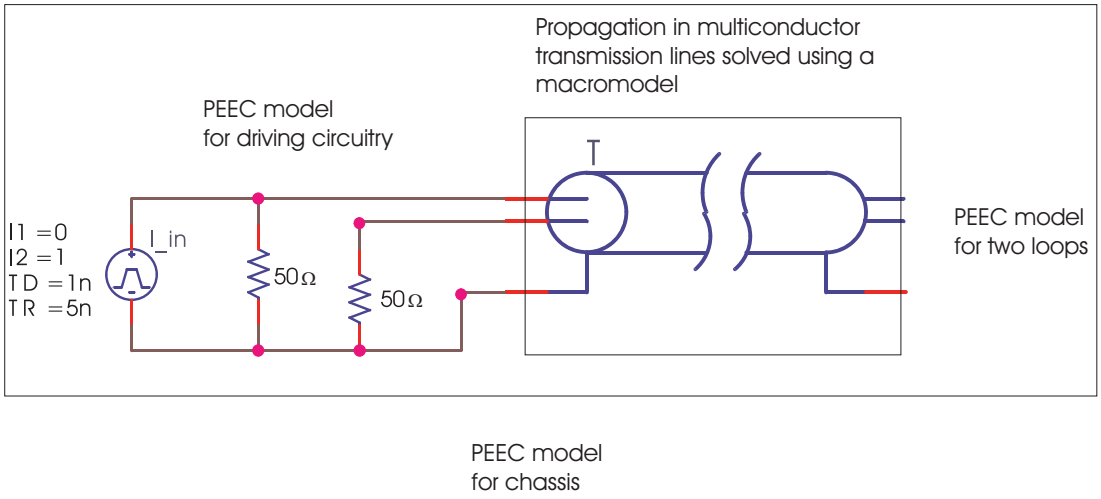

Fig. 5. Test configuration for chassis and interconnect structure.

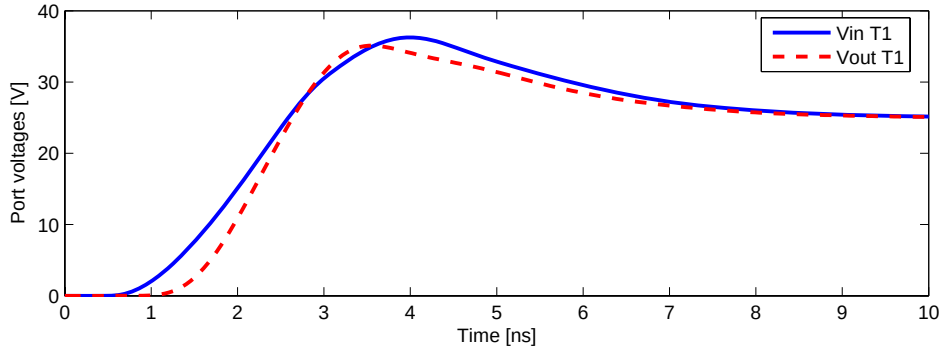

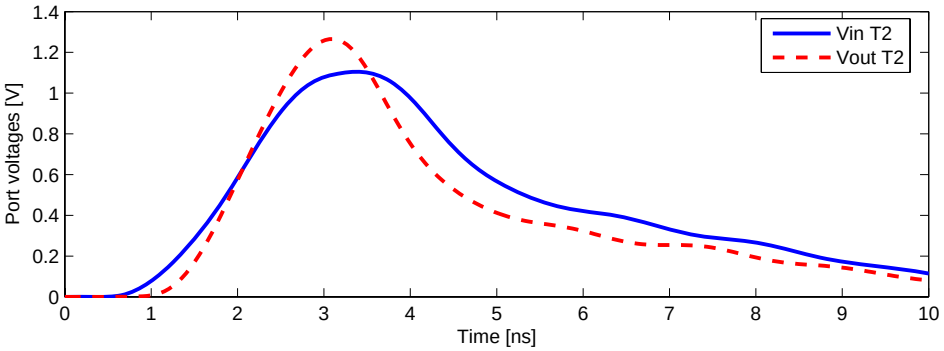

(a)

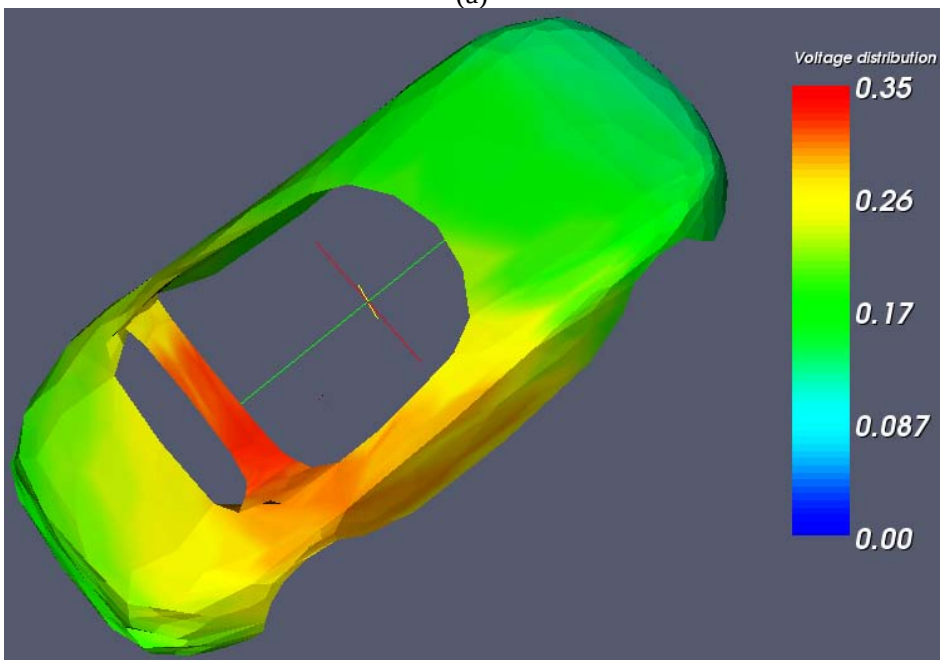

(b)

Fig. 6. MTL port voltages, near and far end, for the chassis and interconnect structure in (a) and induced voltages in the chassis structure (b).

VII. Acknowledgements

The authors would like to thank the Center for Automotive System Technologies and Testing (CASTT) at Luleå University of Technology, Sweden, for its support to this research project.

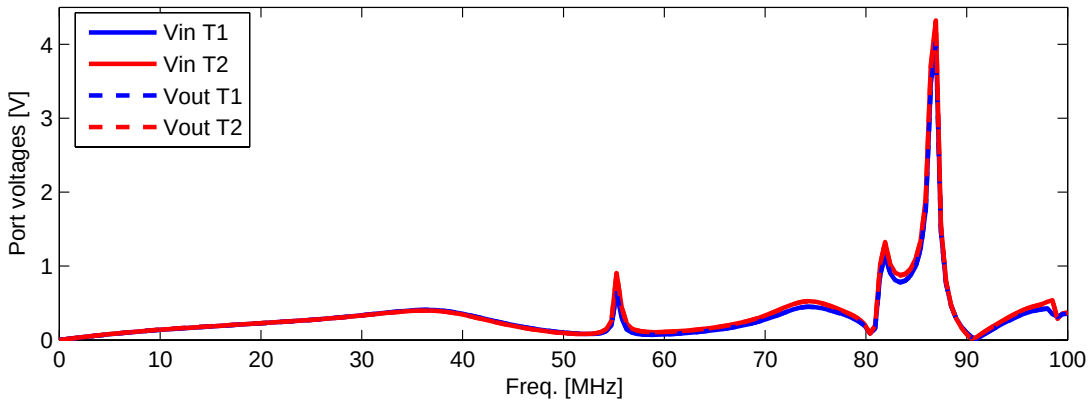

Fig. 7. Induced voltages at interconnect ports from the interaction between the loops and the chassis structure.

REFERENCES

[1] V. Okhmatovski, A. Cangellaris, and J. Morsey, "Accuracy-related issues in electronic modeling of high-speed interconnects", in *Proc. IEEE Int. Symp. EMC*, Boston, MA, 2003, pp. 338-346.

[2] International Technology Roadmap for Semiconductors 2005 edition. [Online]. Available: http://public.itrs.net

[3] A. E. Ruehli, "Inductance calculations in a complex integrated circuit environment", *IBM Journal of Research and Development*, 16(5):470-481, September 1972.

[4] A. E. Ruehli and P. A. Brennan, "Efficient capacitance calculations for three-dimensional multiconductor systems", *IEEE Trans. on Microwave Theory and Techniques*, 21(2):76-82, February 1973.

[5] A. E. Ruehli, "Equivalent circuit models for three-dimensional multiconductor systems", *IEEE Trans. on Microwave Theory and Techniques*, 22(3):216-221, March 1974.

[6] A. E. Ruehli *et al*., "Nonorthogonal PEEC formulation for time- and frequency-domain modeling". *IEEE Trans. on EMC*, 45(2):167-176, May 2003.

[7] G. Wollenberg, A. Göorisch, "Analysis of 3-D interconnect structures with PEEC using SPICE", *IEEE Transactions on Electromagnetic Compatibility*, 41(2):412-417, November 1999.

[8] R. F. Harrington, *Field Computation by Moment Methods*, Macmillan, New York, 1968.

[9] A. W. Glisson and D. R. Wilson, "Simple and Efficient Numerical Methods for Problems of Electromagnetic Radiation and Scattering from Surfaces", *IEEE Tran. on Antennas and Propagation*, vol. 28, pp. 593–603, 1980.

[10] S. M. Rao, D.R. Wilton, and A.W. Glisson, "Electromagnetic scattering by surfaces of arbitrary shape", *IEEE Tran. on Antennas and Propagation* vol. 30, pp. 409–418, 1982.

[11] S. M. Rao and D. R. Wilton, "Transient Scattering by Conducting Surfaces of Arbitrary Shape", *IEEE Tran. on Antennas and Propagation*, vol. 39, pp. 56–61, 1991.

[12] B. M. Kolundzija and B. D. Popovic, "Entire-domain Galerkin method for analysis of metallic antennas and scatterers", *Proceedings of the IEE H*, vol. 140, no. 1, pp. 1–10, 1993.

[13] J. J. H. Wang, *Generalized Moment Method in Electromagnetics*, Wiley, 1991.

[14] S. V. Kochetov, G. Wollenberg, "Stable time domain PEEC solution for pulse excited interconnection structures", in *Proc. of the IEEE Int. Symp. on Electromagnetic Compatibility*, Chicago, USA, 2005.

[15] J. Ekman, G. Antonini and A. E. Ruehli, "Toward Improved Time Domain Stability and Passivity for Full-Wave PEEC Models", in *Proc. of the IEEE Int. Symp. on Electromagnetic Compatibility*, Portland (OR), 2006.

[16] G. Antonini, J. Ekman, and A. E. Ruehli, "Accuracy and Stability Enhancement of PEEC Models for the Time and Frequency Domain", in *Proc. of EMC Europe*, Barcelona, Spain, 2006.

[17] G. Antonini, Deschrijver and T. Dhaene, ”Adaptive Building of Accurate and Stable PEEC Models for EMC Applications”, in *Proc. of EMC Europe 2006 Symposium*, Barcelona, Spain, 2006.

[18] LTU-UAq PEEC Kernel. 2006. [Online]. Available: http://www.csee.ltu.se/peec